University of Cincinnati
Department of Aerospace Engineering & Engineering Mechanics

Fluid-Structure-Interactions of Flexible Panels in Hypersonic Flows

Himakar Ganti, Luis Bravo, Anindya Ghosal, Prashant Khare

AIAA SCITECH 2025

Jan 6th, 2025

Introduction

Introduction

Department of Aerospace Engineering & Engineering Mechanics

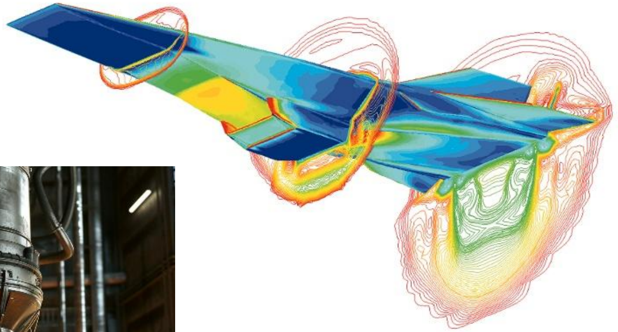

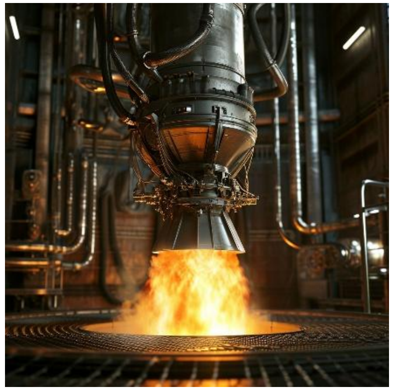

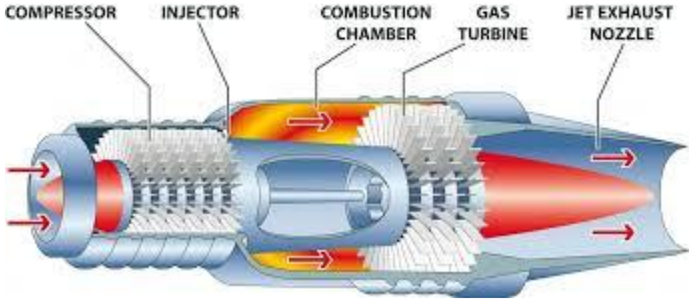

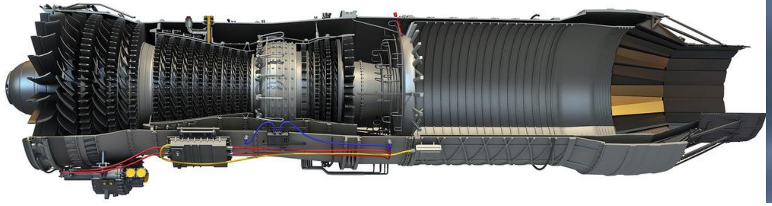

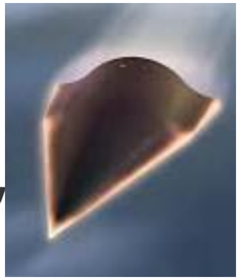

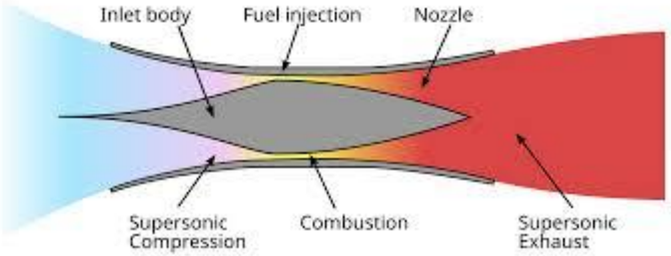

Introduction

- Fluid-Structure-Interactions (FSI) are ubiquitous in nature - wind turbines, biological flows in blood vessels, airflow over race-car tail wings providing downforce, etc.
- FSI in supersonic and hypersonic flows in aerospace engineering – gas turbine engines, ramjet and scramjet engines, solid and liquid-rockets motors, external surfaces of air vehicles.
- Very critical for power-generating equipment- poor design can lead to premature metal fatigue and catastrophic failure.
- FSI simulations capturing transient behavior for hypervelocity flows are very rare and the literature is practically non-existent.
- This provides us with an opportunity to build, develop and use simulations to model and predict transient behavior.
- FSI has two different aspects – physical exchange of pressure forces between fluid and solid and thermal exchange – including both aspects simultaneously is a big challenge.
- Due to inherent challenge of coupling solvers – design and modeling of hypersonic vehicles has been achieved with experiments and static simulations.
- Model simulations are not significantly influential on the design process as static simulations and experimental measurements are time-averaged.

Supersonic Flow, Ma 2.11, over Thin Plate

Department of Aerospace Engineering & Engineering Mechanics

- Unpublished work[1] – FSI conducted for capturing initial-transient and fully-started conditions for supersonic flows over a thin compliant aluminum plate.

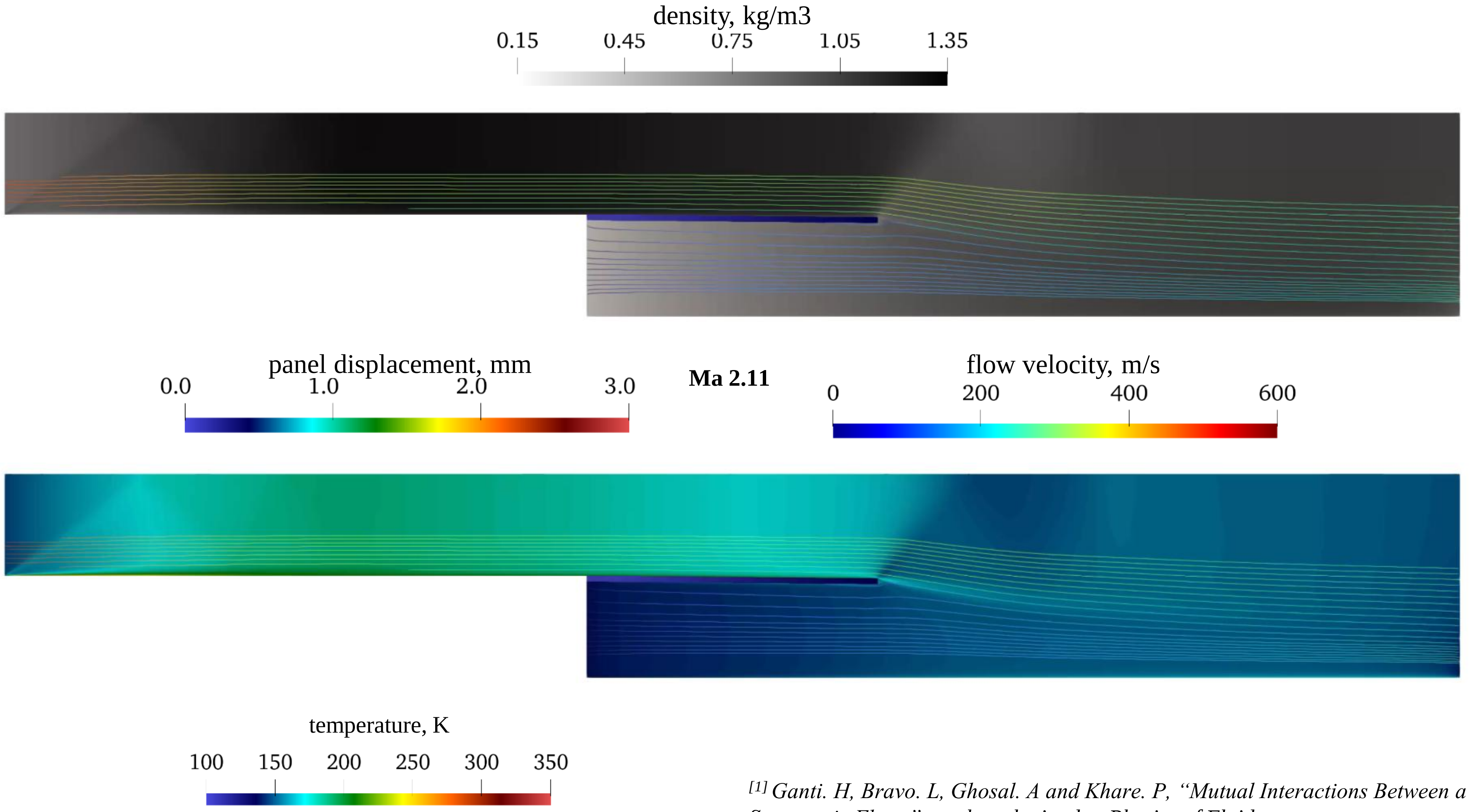

[1] *Ganti. H, Bravo. L, Ghosal. A and Khare. P, "Mutual Interactions Between a Thin Flexible Panel and Supersonic Flows" – to be submitted to Physics of Fluids*

Governing Equations

Governing Equation – Fluid Domain

mass, momentum and energy conservation

$$\mathcal{R}(U) = \frac{\partial U}{\partial t} + \nabla.\bar{F}^c(U) - \nabla.\bar{F}^v(U, \nabla U) - S = 0$$

species reaction rates

$$\dot{w}_s = M_s \sum_r (\beta_{s,r} - \alpha_{s,r})(R_r^f - R_r^b)$$

conserved variables - U convective fluxes - $\bar{F}^c$ viscous fluxes - $\bar{F}^v$ source term - S

$$U = \begin{Bmatrix} \rho_1 \\ \vdots \\ \rho_{n_s} \\ \rho\bar{v} \\ \rho E \\ \rho E_{ve} \end{Bmatrix}, \bar{F}^c = \begin{Bmatrix} \rho_1\bar{v} \\ \vdots \\ \rho_{n_s}\bar{v} \\ \rho_1\bar{v}\otimes\bar{v} + \bar{\bar{I}}p \\ \rho E\bar{v} + p\bar{v} \\ \rho E_{ev}\bar{v} \end{Bmatrix}, \bar{F}^v = \begin{Bmatrix} -\bar{J}_1 \\ \vdots \\ -\bar{J}_{n_s} \\ \bar{\bar{\tau}} \\ \bar{\bar{\tau}}.\bar{v} + \sum_k \kappa_k \nabla T_k - \sum_s \bar{J}_s h_s \\ \kappa_{ve}\nabla T_{ve} - \sum_s \bar{J}_s E_{ve} \end{Bmatrix}, S = \begin{Bmatrix} \dot{w}_1 \\ \vdots \\ \dot{w}_{n_s} \\ 0 \\ 0 \\ \dot{\theta}_{tr:ve} + \sum_s \dot{w}_s E_{ve,s} \end{Bmatrix}$$

two temperature model

$$\rho e = \sum_s \rho_s \left(e_s^{tr} + e_s^{rot} + e_s^{vib} + e_s^{el} + e_s^{o} + \frac{1}{2}\bar{v}^T\bar{v} \right)$$

$$\rho e^{ve} = \sum_s \rho_s \left(e_s^{vib} + e_s^{el} \right)$$

molecular viscosity

$$\mu = \mu_0 \left(\frac{T}{T_0} \right)^{3/2} \left(\frac{T_0 + S_\mu}{T + S_\mu} \right)$$

Governing Equation – Hypersonic Flow Modeling

two temperature model

$$\rho e = \sum_s \rho_s \left(e_s^{tr} + e_s^{rot} + e_s^{vib} + e_s^{el} + e_s^{o} + \frac{1}{2}\bar{v}^T \bar{v} \right)$$

$$\rho e^{ve} = \sum_s \rho_s \left(e_s^{vib} + e_s^{el} \right)$$

$$e_s^{tr} = \begin{cases} \frac{3}{2}\frac{R}{M_s}T, & \text{for monatomic and polyatomic species,} \\ 0, & \text{for electrons} \end{cases}$$

$$e_s^{rot} = \begin{cases} \frac{\xi}{2}\frac{R}{M_s}T, & \text{for polyatomic species,} \\ 0, & \text{for monatomic species and electrons} \end{cases}$$

$$e_s^{vib} = \begin{cases} \frac{R}{M_s}\frac{\theta_s^{\text{vib}}}{\left(e^{\left(\theta_s^{\text{vib}}/T_{ve}\right)} - 1\right)}, & \text{for polyatomic species,} \\ 0, & \text{for monatomic species and electrons} \end{cases}$$

$$e_s^{el} = \begin{cases} \frac{R}{M_s}\frac{\sum_{i=1}^{\infty} g_{i,s}\theta_{i,s}^{el}\exp\left(-\theta_{i,s}^{el}/T_{ve}\right)}{\sum_{i=1}^{\infty} g_{i,s}\exp\left(-\theta_{i,s}^{el}/T_{ve}\right)}, & \text{for monatomic and polyatomic species,} \\ \frac{3}{2}\frac{R}{M_s}T^{ve}, & \text{for electrons} \end{cases}$$

Millikan and White relaxation, with high temperature limit correction

$$\tau_{sr} = \frac{1}{p}\exp\left[A_s r\left(T^{-1/3} - 0.015\mu_{sr}^{1/4}\right) - 18.42\right]$$

$$\tau_{ps} = \frac{1}{\sigma_s c_s n}$$

Landau-Teller relaxation, with Park limit

$$\dot{\theta}_{tr:ve} = \sum_s \rho_s \frac{dE_{ve,s}}{dt} = \sum_s \rho_s \frac{E_{ve*,s} - E_{ve,s}}{\tau_s}$$

Governing Equations - Solid Domain

Elasticity Equation with Geometric Non-Linearities

$$\rho_s \frac{\partial^2 \mathbf{u}}{\partial t^2} = \nabla\left(\mathbf{F}\cdot\mathbf{S}\right) + \rho_s f \qquad \begin{cases} \mathrm{u}_s = \mathrm{u}_{s,e} & \text{on } \Gamma_{s,e} \\ \sigma_s \mathrm{n}_s = \lambda_{s,n} & \text{on } \Gamma_{s,n} \end{cases}$$

Second Piola-Kirchoff Stress

$$S^{PK}{}_{ij} = \lambda_s E_{kk}\delta_{ij} + 2\mu_s E_{ij}$$

Lagrangian Stress Tensor

$$E_{ij} = \frac{1}{2}\left(\frac{\partial u_i}{\partial x_j} + \frac{\partial u_j}{\partial x_i}\right) + \frac{1}{2}\frac{\partial u_k}{\partial x_i}\frac{\partial u_k}{\partial x_j}$$

Young's Modulus in terms of Lame's Constant

$$E = \frac{\mu_s\left(3\lambda_s + 2\mu_s\right)}{\lambda_s + \mu_s}$$

Poisson's Ratio in terms of Lame's Constant

$$\nu = \frac{\lambda_s}{2\left(\lambda_s + \mu_s\right)}$$

Governing Equations – Interface Coupling

Boundary velocity is same as velocity of solid or fluid at the boundary $u_f = u_s = u_\Gamma$

Equilibrium at the interface gives $\lambda_f + \lambda_s = 0$

The Dirichlet-Neumann non-linear condition for the fluid $\lambda_f = F_f\left(u_{\Gamma_f}\right) \text{ on } \Gamma_{f,i}$

The Dirichlet-Neumann non-linear condition for the solid $\lambda_s = F_s\left(u_{\Gamma_s}\right) \text{ on } \Gamma_{s,n}$

Steklov-Poincare equations

$$F_f\left(u_\Gamma\right) + F_s\left(u_\Gamma\right) = 0$$

$$F_s^{-1}\left(-F_f\left(u_\Gamma\right)\right) = u_\Gamma$$

Model Validation

Experimental Validation – Configuration & Conditions

- The 25° -55° double cone configuration of CUBRC[1] Run 80 is selected for hypersonic flow validation.
- Double-cone geometry with freestream conditions is shown below.
- A mesh with a uniform grid size of 200 μm was generated for simulating the hypersonic flow.
- ROE scheme for spatial, with 4th order Runge-Kutta time marching scheme were selected for the simulation with a timestep of 1.0E-8 s.
- The double cone surface is considered isothermal at 300 K.
- Vibrational temperature was set at 2711 for the two-temperature model used for hypersonic flows.
- Chemical reactions were not modeled for the 2-species (N_2, N) working fluid.

CUBRC Run 80 Flow Conditions		
2-species Nitrogen		
Mach #		11.850
Gamma		1.4
R	J/kg-K	288.68
Vibration Temperature	K	2711.00
Total Pressure	Pa	8438645
Total Temperature	K	4828.0
Temperature	K	166.00
Pressure	Pa	63.60
Density	kg/m3	1.3272E-03
Velocity	m/s	3069.34
Viscosity @ 273 K	Pa-s	1.173E-05
Length	m	1.000
Reynolds # (Integral)		347279
Kolmogorov Scale	μm	70.0
Taylor Scale Reynolds		1522
Taylor Scale	m	5.366E-03
Sutherland Temperature	K	110.4
Actual Viscosity	Pa-s	7.710E-06

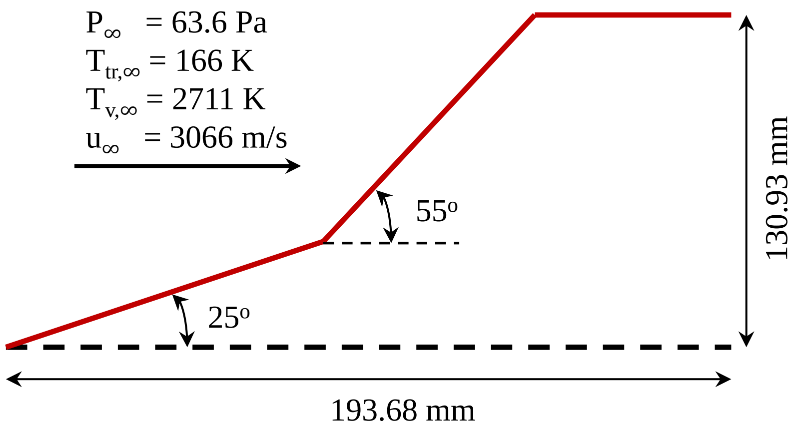

[1] *Holden. M, "The LENS Facilities and Experimental Studies to Evaluate the Modeling of Boundary Layer Transition, Shock/Boundary Layer Interaction, Real Gas, Radiation and Plasma Phenomena in Contemporary CFD Codes"* Report, 2010. URL https://apps.dtic.mil/sti/citations/ADA581907.

Experimental Validation - Pressure

- SU2 validation results with the experiment CUBRC [1] Run 80.

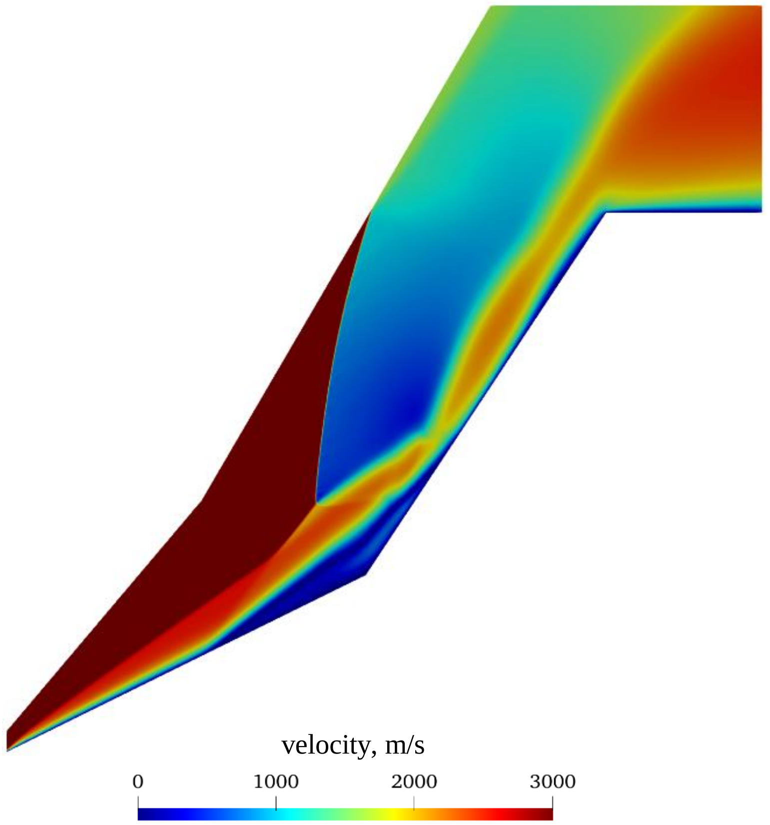

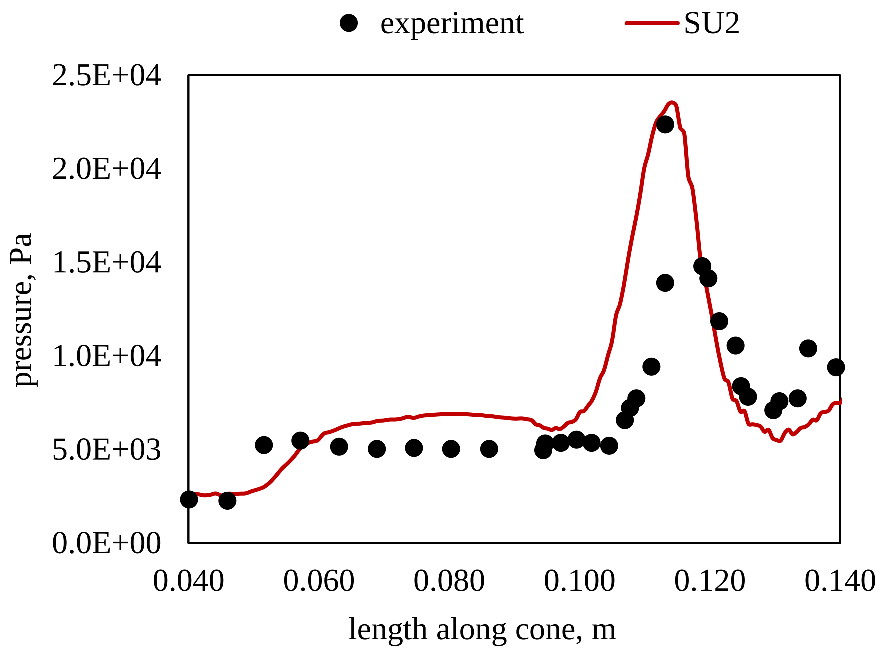

[1] *Holden. M, "The LENS Facilities and Experimental Studies to Evaluate the Modeling of Boundary Layer Transition, Shock/Boundary Layer Interaction, Real Gas, Radiation and Plasma Phenomena in Contemporary CFD Codes"* Report, 2010. URL https://apps.dtic.mil/sti/citations/ADA581907.

Initial Transients – Flow Behavior

Thin Panel – Configuration & Conditions

- The HyMAX [1] configuration of UNSW was selected for operating conditions.
- Simulations are run for an initial transient time of 20 ms.
- Flow domain has a uniform mesh size of 200 µm.
- Solid domain has a uniform mesh size of 200 µm.
- Plate thickness is 2.0 mm
- 5-species air with the following - N_2, O_2, N, O, NO; is the working fluid.
- Turbulence is not modeled as the grid size is 200 µm, which is a coarse DNS resolution with the Kolmogorov scale estimated for the high-speed flow at 80 µm.

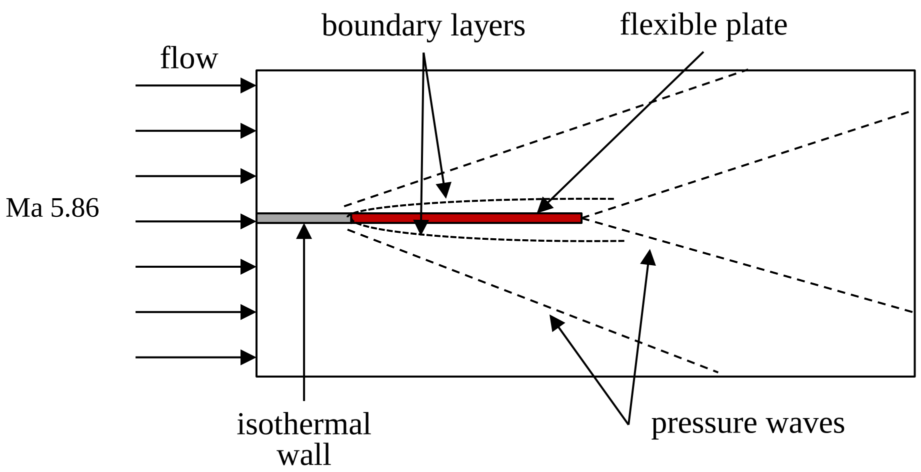

Flow Conditions		
5-species Air		
Mach #		5.86
Gamma		1.4
R	J/kg-K	288.68
Total Pressure	Pa	1.008E+06
Total Temperature	K	600
Vibration Temperature	K	2711
Temperature	K	76.26
Pressure	Pa	737.8
Density	kg/m3	0.03352
Velocity	m/s	1028.765
Viscosity @ 273 K	Pa-s	1.173E-05
Length	m	0.13
Reynolds # (Integral)		382123
Kolmogorov Scale	µm	80.0
Taylor Scale Reynolds		1596
Taylor Scale	m	6.650E-04
Sutherland Temperature	K	110.4
Actual Viscosity	Pa-s	3.551E-06

[1] Poudel, N., Sahani, S., Pudasaini, S., Bhattrai, S., Darlami, K., and Talluru, M. K., "Numerical Study of Hypersonic Fluid-Structure Interaction on a Cantilevered PlateWith Shock Impingement Using Low and High-Fidelity Numerical Methods," AIAA AVIATION FORUM AND ASCEND 2024, American Institute of Aeronautics and Astronautics, 2024. doi:10.2514/6.2024-4053,

University of CINCINNATI

Initial Transient Flow – Pressure

Department of Aerospace Engineering & Engineering Mechanics

- Pressure evolution for a rigid, steel and aluminum plates for initial 20 ms.
- Rigid plate does not have a stagnation region, while the steel and aluminum plate show stagnation regions at the free end of the thin plate.
- A vortex street originates at the tip of the rigid plate but is eventually dissipated.
- Standing shock waves originating from the stagnation region at the plate tip are more significant for the flexible steel and aluminum plates when compared to the rigid plate.
- Aluminum plate has larger tip displacements, at 3.0 mm; Steel has lower tip displacements at 1.0 mm.

thin plate displacement, mm

steel plate

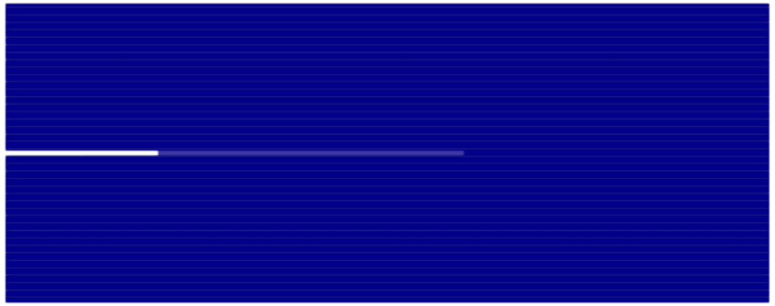

rigid plate

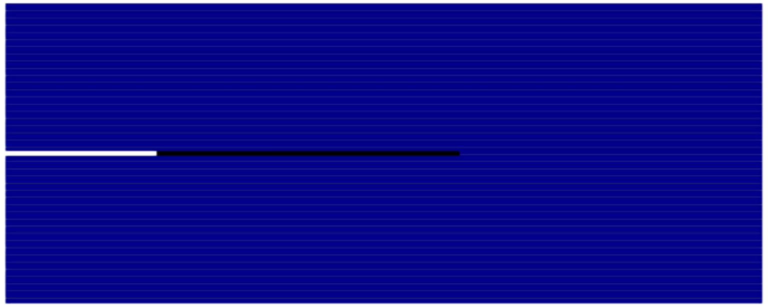

pressure, Pa

velocity, m/s

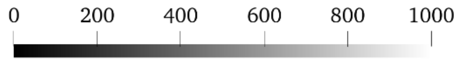

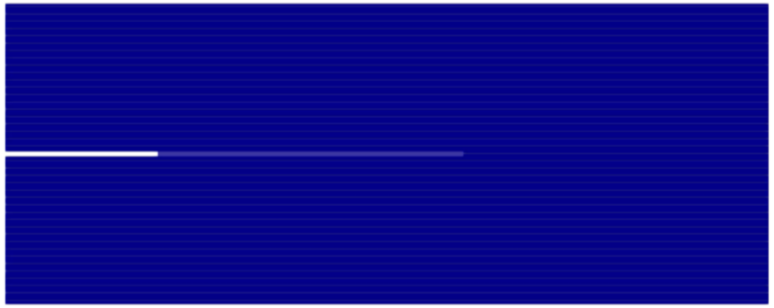

aluminum plate

thin plate displacement, mm

Time Averaged Flow - Pressure

- The standing shock waves originating at the tip of the steel and aluminum plates have larger pressure gradients.
- The rigid plate has no stagnation region, while the steel and aluminum plates have stagnation regions attached to the thin plate tip.
- Vortex shedding phenomenon is not observed for time-averaged pressure.

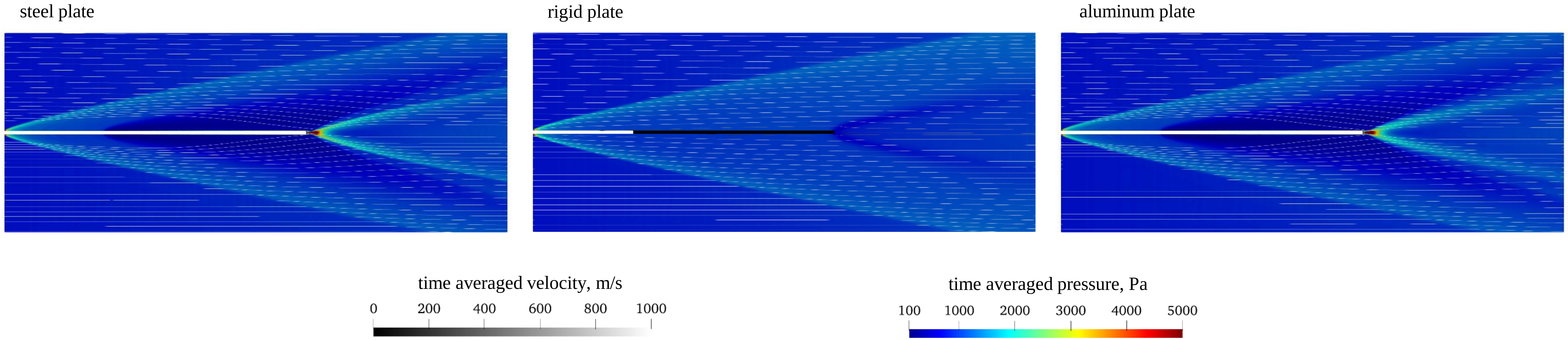

Initial Transient Flow – Temperature

- Temperature evolution for a rigid, steel and aluminum plates for initial 20 ms.
- For the rigid plate, a vortex street type formation is observed, which is not present with the other plates.
- A thermal boundary layer is formed around the rigid plate, while a thermal boundary layer is not visible for the steel or aluminum plates.
- The presence of a vortex street structure suggests the possibility of transitioning to higher vorticity with sustained flow.

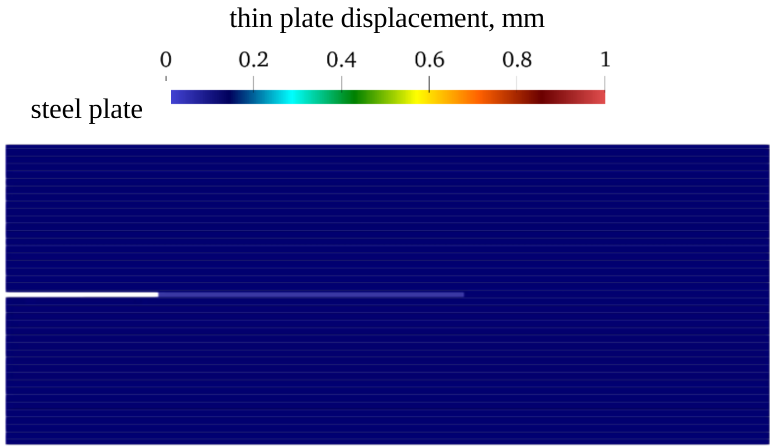

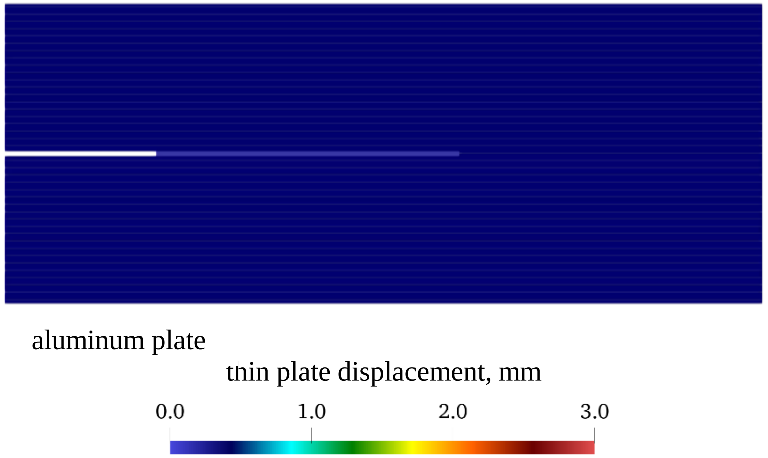

Time Averaged Flow - Temperature

- The standing shock waves originating at the tip of the steel and aluminum plates have larger pressure gradients.
- The rigid plate has no stagnation region, while the steel and aluminum plates have stagnation regions attached to the thin plate tip.
- Vortex shedding phenomenon is not observed for time-averaged pressure.

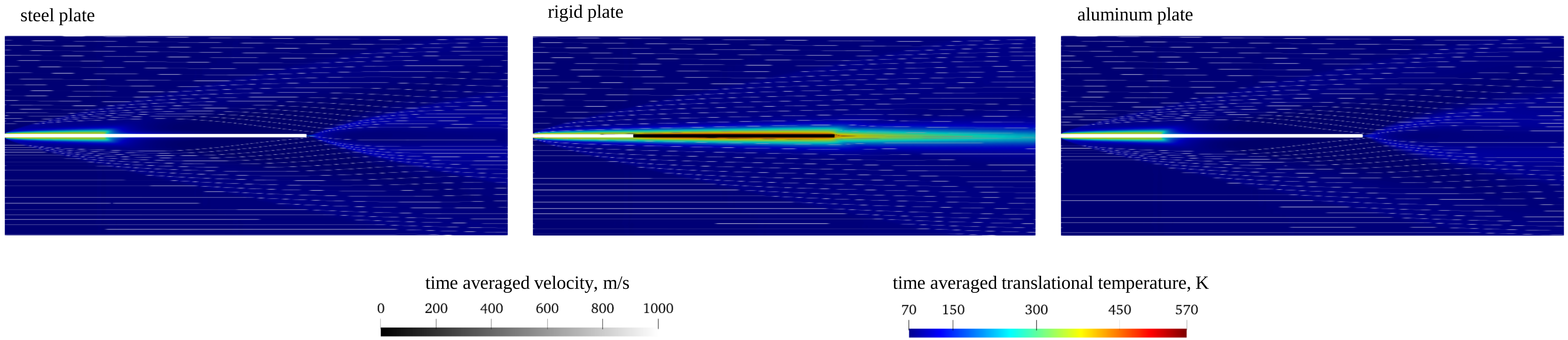

University of CINCINNATI

Initial Transient Flow – Vorticity

Department of Aerospace Engineering & Engineering Mechanics

- Vorticity evolution for a rigid, steel and aluminum plates for initial 20 ms.
- Vorticity extends along the edges of the rigid plate but gets dissipated due to steel and aluminum plate oscillations.
- Vorticity is the highest along the wall edges before it interacts with steel and aluminum plates.
- Rigid plate configuration has a boundary layer with high vorticity.

thin plate displacement, mm

0 0.2 0.4 0.6 0.8 1

steel plate

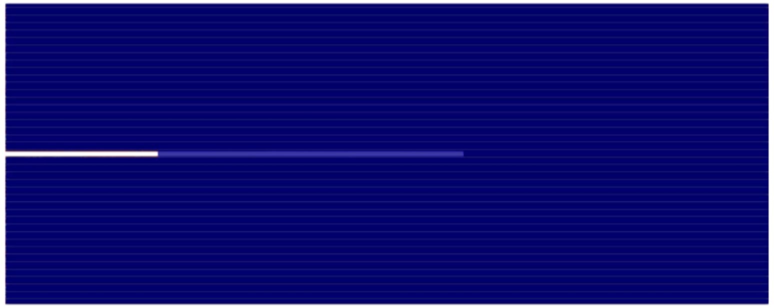

rigid plate

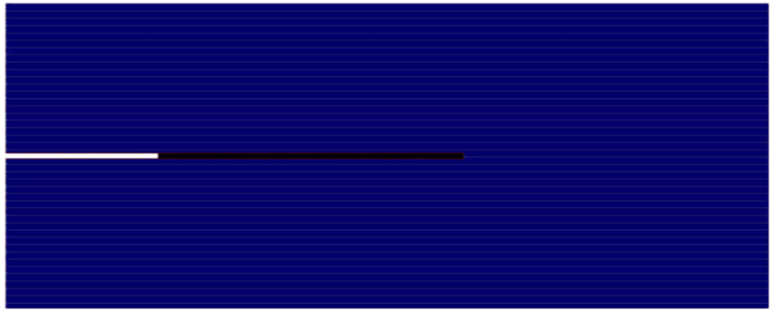

vorticity, rad/s

0 20000 40000 60000 80000 100000

velocity, m/s

0 200 400 600 800 1000

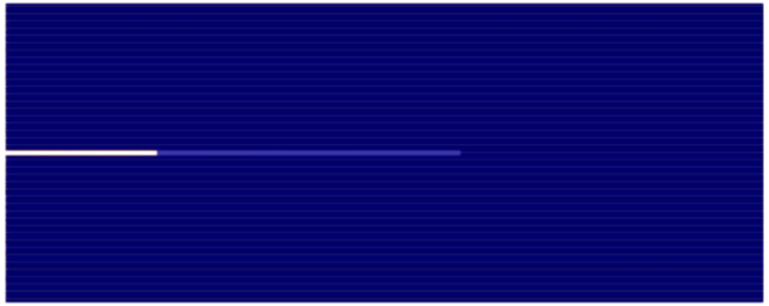

aluminum plate

thin plate displacement, mm

0.0 1.0 2.0 3.0

Time Averaged Flow - Vorticity

- The rigid plate has the highest vorticity around the plate edges, and this is extended downstream of the rigid plate tip.
- Steel and aluminum plate do not see an accumulation of vorticity as their oscillations tends to dissipate the vorticity which is confined to the walls connected before the plates.
- Transition of flow to turbulence is not complete and longer simulation times can reveal the changes to vorticity.

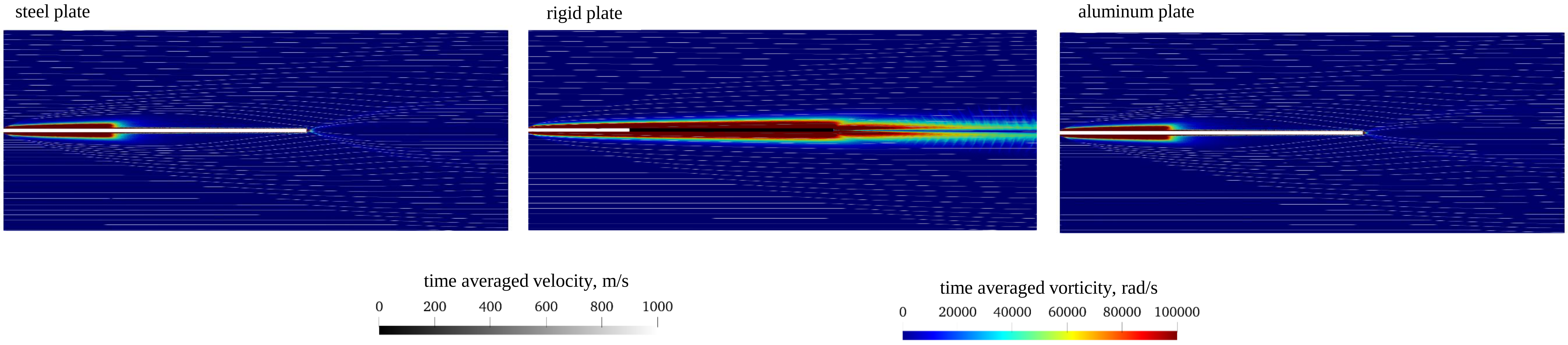

Initial Transient Flow – Q-criterion

- Q-criterion evolution for a rigid, steel and aluminum plates for initial 20 ms.
- Shear dominates in the wake region between the standing shock waves for steel and aluminum plates.
- For the rigid plate configuration, vorticity is dominant close to the plate edges and showing up as a thick boundary layer. This implies that the flow in the boundary layer has very high vorticity.
- Vortex shedding and the vortex street is visible for the rigid plate.

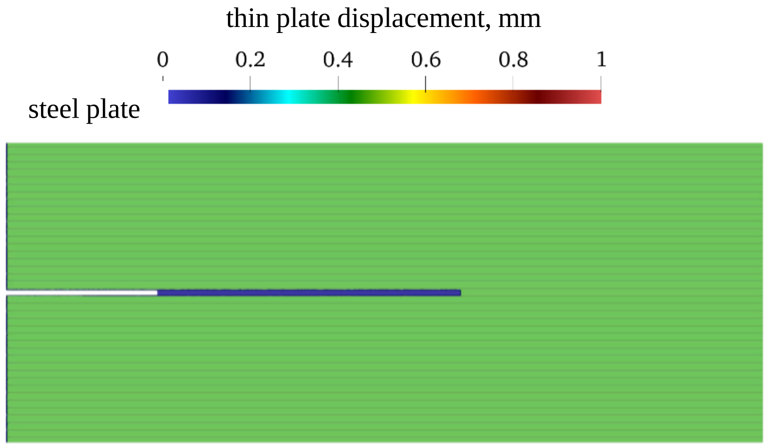

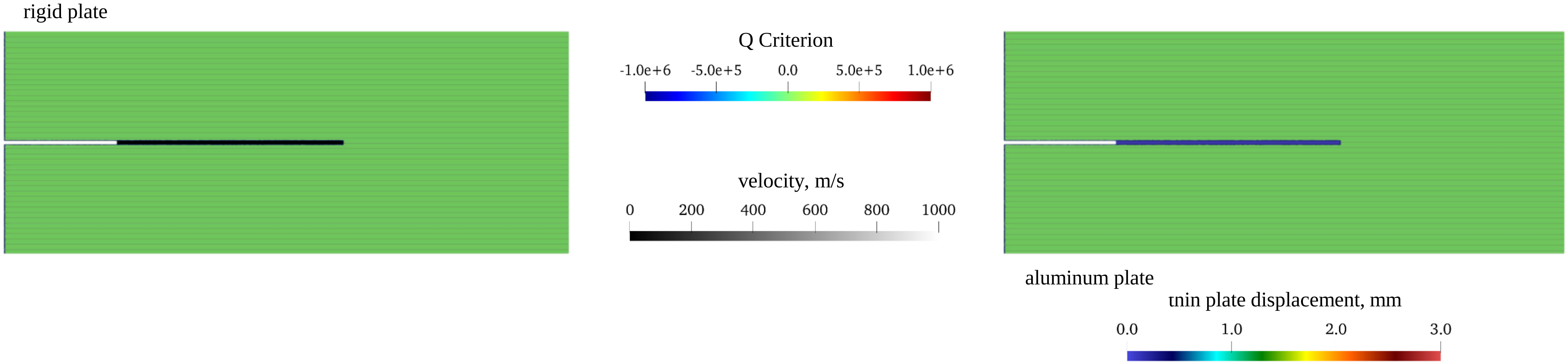

Time Averaged Flow – Q-Criterion

- The rigid plate has the highest vorticity around the plate edges, and this is extended downstream of the rigid plate tip.
- Steel and aluminum plate do not see an accumulation of vorticity as their oscillations tends to dissipate the vorticity which is confined to the walls connected before the plates.
- Transition of flow to turbulence is not complete and longer simulation times can reveal the changes to vorticity.

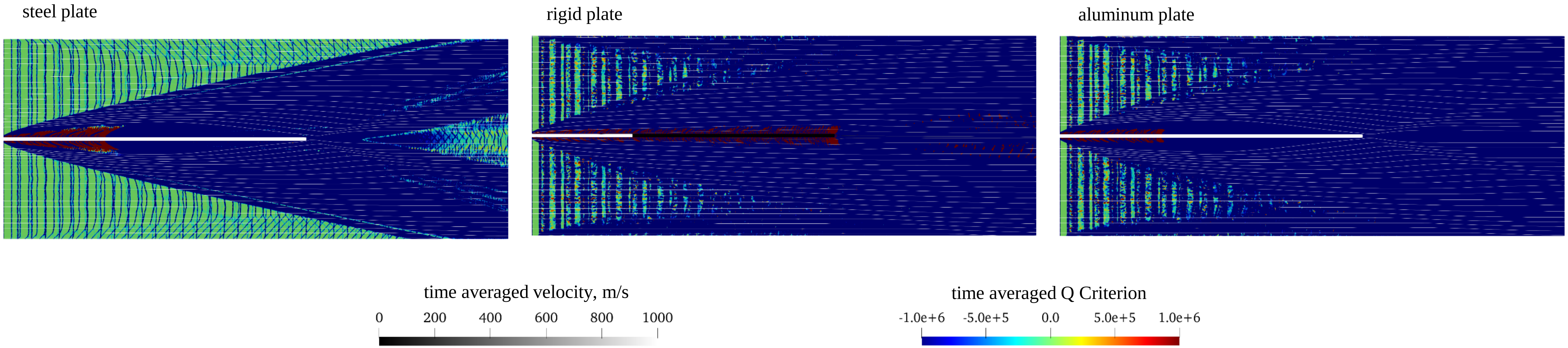

Initial Transients – Solid Behavior

University of CINCINNATI

Time Averaged Displacement and Stress

Department of Aerospace Engineering & Engineering Mechanics

- Steel and aluminum plates both show the same time-averaged displacement at ~ 0.2 mm.
- The thin plates experience maximum stress at the clamped end.
- Von Mises stress for - steel plate ~ 16 Mpa; aluminum plate ~ 17 MPa.
- Maximum tip displacement amplitude for - steel plate ~ 1 mm; aluminum plate ~ 3mm.
- The steel plate has a smaller tip displacement amplitude when compared to the tip displacement amplitude of the aluminum plate.
- The frequency of oscillation for the tip of the - steel plate is 137 Hz; aluminum plate is 183 Hz.

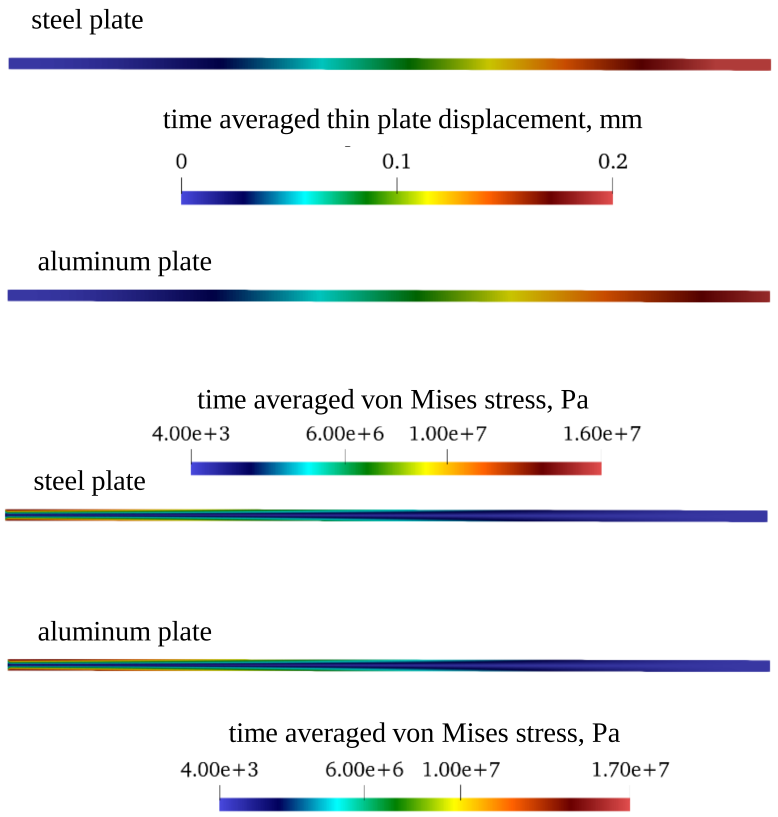

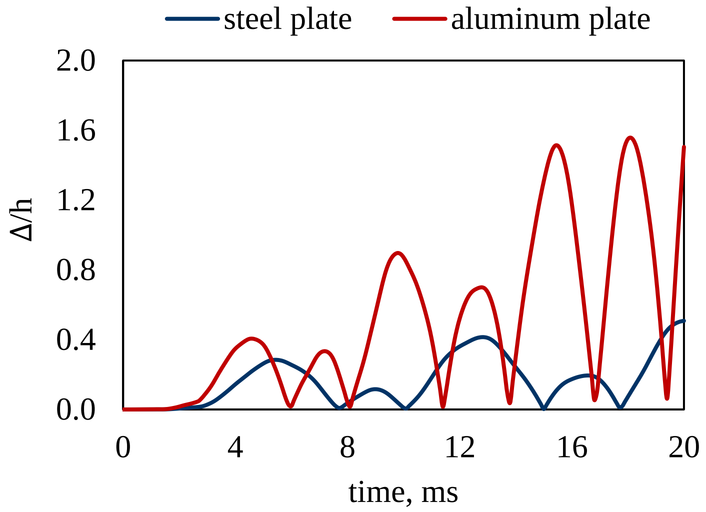

Conclusions & Future Work

Conclusions & Future Work

Conclusions:

- Rigid, steel and aluminum plates were simulated for interactions with hypersonic flows, for initial transient behavior of 20 ms.
- Transient and time-averaged fluid and solid quantities were both reported to provide more information for design decisions.
- Shock waves at the plate tip for steel and aluminum plates have larger pressure gradients.
- The flow behavior for the rigid plate configuration is different than the flow behavior for steel and aluminum plate behavior.
- The aluminum plate has higher displacement amplitudes and oscillation frequency when compared to the steel plate due to the lower elasticity.

Future Work:

- Simulations will be run for longer times to investigate change is flow and solid behavior and fluid-structure interactions.
- Different flow conditions and solid plate materials can be examined for fluid-structure-interactions under hypersonic flow conditions.

Questions